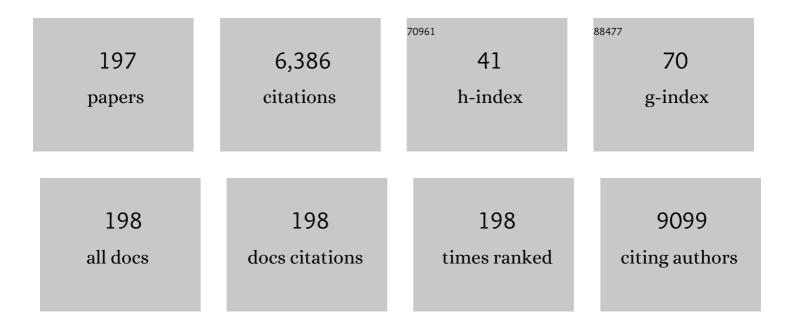
Jose Angel Martin-Gago

List of Publications by Year in descending order

Source: https://exaly.com/author-pdf/8456253/publications.pdf Version: 2024-02-01



#	Article	IF	CITATIONS
1	Direct growth of graphene-MoS2 heterostructure: Tailored interface for advanced devices. Applied Surface Science, 2022, 581, 151858.	3.1	16
2	Steering Hydrocarbon Selectivity in CO ₂ Electroreduction over Soft-Landed CuO _{<i>x</i>} Nanoparticle-Functionalized Gas Diffusion Electrodes. ACS Applied Materials & Interfaces, 2022, 14, 2691-2702.	4.0	9
3	On-Surface Thermal Stability of a Graphenic Structure Incorporating a Tropone Moiety. Nanomaterials, 2022, 12, 488.	1.9	2
4	Copper-assisted oxidation of catechols into quinone derivatives. Chemical Science, 2021, 12, 2257-2267.	3.7	16
5	Role of the Structure and Reactivity of Cu and Ag Surfaces in the Formation of a 2D Metal–Hexahydroxytriphenylene Network. Journal of Physical Chemistry C, 2021, 125, 17333-17341.	1.5	12
6	LiCl Photodissociation on Graphene: A Photochemical Approach to Lithium Intercalation. ACS Applied Materials & Interfaces, 2021, 13, 42205-42211.	4.0	2
7	Few-layer antimonene electrical properties. Applied Materials Today, 2021, 24, 101132.	2.3	6
8	Silicon and Hydrogen Chemistry under Laboratory Conditions Mimicking the Atmosphere of Evolved Stars. Astrophysical Journal, 2021, 906, 44.	1.6	10
9	Metal-catalyst-free gas-phase synthesis of long-chain hydrocarbons. Nature Communications, 2021, 12, 5937.	5.8	7
10	Tailored graphenic structures directly grown on titanium oxide boost the interfacial charge transfer. Applied Surface Science, 2020, 504, 144439.	3.1	4
11	Prevalence of non-aromatic carbonaceous molecules in the inner regions of circumstellar envelopes. Nature Astronomy, 2020, 4, 97-105.	4.2	48
12	Oxygen intercalation in PVD graphene grown on copper substrates: A decoupling approach. Applied Surface Science, 2020, 529, 147100.	3.1	10
13	On‣urface Driven Formal Michael Addition Produces m â€Polyaniline Oligomers on Pt(111). Angewandte Chemie - International Edition, 2020, 59, 23220-23227.	7.2	5
14	On‣urface Driven Formal Michael Addition Produces m â€₽olyaniline Oligomers on Pt(111). Angewandte Chemie, 2020, 132, 23420-23427.	1.6	1
15	Role of the Metal Surface on the Room Temperature Activation of the Alcohol and Amino Groups of <i>p</i> -Aminophenol. Journal of Physical Chemistry C, 2020, 124, 19655-19665.	1.5	2
16	Chemically synthesized chevron-like graphene nanoribbons for electrochemical sensors development: determination of epinephrine. Scientific Reports, 2020, 10, 14614.	1.6	40
17	The Chemistry of Cosmic Dust Analogs from C, C ₂ , and C ₂ H ₂ in C-rich Circumstellar Envelopes. Astrophysical Journal, 2020, 895, 97.	1.6	30
18	Chemical equilibrium in AGB atmospheres: successes, failures, and prospects for small molecules, clusters, and condensates. Astronomy and Astrophysics, 2020, 637, A59.	2.1	55

#	Article	IF	CITATIONS
19	Production and processing of graphene and related materials. 2D Materials, 2020, 7, 022001.	2.0	333
20	INFRA-ICE: An ultra-high vacuum experimental station for laboratory astrochemistry. Review of Scientific Instruments, 2020, 91, 124101.	0.6	2
21	Ultra-thin NaCl films as protective layers for graphene. Nanoscale, 2019, 11, 16767-16772.	2.8	6
22	Broad-band high-resolution rotational spectroscopy for laboratory astrophysics. Astronomy and Astrophysics, 2019, 626, A34.	2.1	15
23	Hydrogen quenches the size effects in carbon clusters. Physical Chemistry Chemical Physics, 2019, 21, 10402-10410.	1.3	3
24	Direct visualization of the native structure of viroid RNAs at single-molecule resolution by atomic force microscopy. RNA Biology, 2019, 16, 295-308.	1.5	17
25	Reversible graphene decoupling by NaCl photo-dissociation. 2D Materials, 2019, 6, 025021.	2.0	8
26	Versatile Graphene-Based Platform for Robust Nanobiohybrid Interfaces. ACS Omega, 2019, 4, 3287-3297.	1.6	9
27	Differential pulse voltammetric determination of the carcinogenic diamine 4,4′-oxydianiline by electrochemical preconcentration on a MoS2 based sensor. Mikrochimica Acta, 2019, 186, 793.	2.5	8
28	Morphology Clustering Software for AFM Images, Based on Particle Isolation and Artificial Neural Networks. IEEE Access, 2019, 7, 160304-160323.	2.6	2
29	Fluorescence enhancement of fungicide thiabendazole by van der Waals interaction with transition metal dichalcogenide nanosheets for highly specific sensors. Nanoscale, 2019, 11, 23156-23164.	2.8	6
30	On-Surface Hydrogen-Induced Covalent Coupling of Polycyclic Aromatic Hydrocarbons via a Superhydrogenated Intermediate. Journal of the American Chemical Society, 2019, 141, 3550-3557.	6.6	40
31	Structural characterization of as-grown and quasi-free standing graphene layers on SiC. Applied Surface Science, 2019, 466, 51-58.	3.1	8
32	Modelling of adsorption and intercalation of hydrogen on/into tungsten disulphide multilayers and multiwall nanotubes. Physical Chemistry Chemical Physics, 2018, 20, 12061-12074.	1.3	6
33	Chemistry below graphene: Decoupling epitaxial graphene from metals by potential-controlled electrochemical oxidation. Carbon, 2018, 129, 837-846.	5.4	30
34	Enantiopure distorted ribbon-shaped nanographene combining two-photon absorption-based upconversion and circularly polarized luminescence. Chemical Science, 2018, 9, 3917-3924.	3.7	132
35	Reversible Thermochromic Polymeric Thin Films Made of Ultrathin 2D Crystals of Coordination Polymers Based on Copper(I)â€Thiophenolates. Advanced Functional Materials, 2018, 28, 1704040.	7.8	53

Adsorption and Self-Assembly of Organic Molecules on TiO2 Substrates. , 2018, , 1-12.

2

#	Article	IF	CITATIONS
37	Using radio astronomical receivers for molecular spectroscopic characterization in astrochemical laboratory simulations: A proof of concept. Astronomy and Astrophysics, 2018, 609, A15.	2.1	12
38	Circumstellar chemistry of Si-C bearing molecules in the C-rich AGB star IRC+10216. Proceedings of the International Astronomical Union, 2018, 14, 535-537.	0.0	4
39	Size-Selective Carbon Clusters as Obstacles to Graphene Growth on a Metal. Nano Letters, 2018, 18, 4812-4820.	4.5	7
40	Onâ€Surface Bottomâ€Up Synthesis of Azine Derivatives Displaying Strong Acceptor Behavior. Angewandte Chemie, 2018, 130, 8718-8722.	1.6	7
41	Onâ€Surface Bottomâ€Up Synthesis of Azine Derivatives Displaying Strong Acceptor Behavior. Angewandte Chemie - International Edition, 2018, 57, 8582-8586.	7.2	13
42	Precisely controlled fabrication, manipulation and in-situ analysis of Cu based nanoparticles. Scientific Reports, 2018, 8, 7250.	1.6	27
43	Atomically-resolved edge states on surface-nanotemplated graphene explored at room temperature. Nanoscale, 2017, 9, 3905-3911.	2.8	3
44	Growth of carbon chains in IRC +10216 mapped with ALMA. Astronomy and Astrophysics, 2017, 601, A4.	2.1	60
45	Highly selective covalent organic functionalization of epitaxial graphene. Nature Communications, 2017, 8, 15306.	5.8	45
46	High-quality PVD graphene growth by fullerene decomposition on Cu foils. Carbon, 2017, 119, 535-543.	5.4	29
47	Chemisorption of Pentacene on Pt(111) with a Little Molecular Distortion. Journal of Physical Chemistry C, 2017, 121, 22797-22805.	1.5	17
48	Spectroscopic characterization of the on-surface induced (cyclo)dehydrogenation of a N-heteroaromatic compound on noble metal surfaces. Physical Chemistry Chemical Physics, 2017, 19, 22454-22461.	1.3	3
49	Unveiling universal trends for the energy level alignment in organic/oxide interfaces. Physical Chemistry Chemical Physics, 2017, 19, 24412-24420.	1.3	9
50	Identification of PAH Isomeric Structure in Cosmic Dust Analogs: The AROMA Setup. Astrophysical Journal, 2017, 843, 34.	1.6	29
51	Role of the Pinning Points in epitaxial Graphene Moir $ ilde{A}$ © Superstructures on the Pt(111) Surface. Scientific Reports, 2016, 6, 20354.	1.6	18
52	Controlled injection of a liquid into ultra-high vacuum: Submonolayers of adenosine triphosphate deposited on Cu(110). Journal of Applied Physics, 2016, 120, 145307.	1.1	3
53	Metalation of tetraphenylporphyrin with nickel on a TiO2(110)-1 × 2 surface. Nanoscale, 2016, 8, 1123-1132.	2.8	20
54	Adsorption and coupling of 4-aminophenol on Pt(111) surfaces. Surface Science, 2016, 646, 5-12.	0.8	8

#	Article	IF	CITATIONS
55	Mimicking Martian dust: An in-vacuum dust deposition system for testing the ultraviolet sensors on the Curiosity rover. Review of Scientific Instruments, 2015, 86, 105113.	0.6	9
56	Electrical Conductivity and Strong Luminescence in Copper Iodide Double Chains with Isonicotinato Derivatives. Chemistry - A European Journal, 2015, 21, 17282-17292.	1.7	31
57	A magnesium-induced RNA conformational switch at the internal ribosome entry site of hepatitis C virus genome visualized by atomic force microscopy. Nucleic Acids Research, 2015, 43, 565-580.	6.5	23
58	On-surface self-organization of a robust metal–organic cluster based on copper(<scp>i</scp>) with chloride and organosulphur ligands. Chemical Communications, 2015, 51, 3243-3246.	2.2	4
59	Graphene growth on Pt(111) and Au(111) using a MBE carbon solid-source. Diamond and Related Materials, 2015, 57, 58-62.	1.8	27
60	Densely Packed Perylene Layers on the Rutile TiO ₂ (110)-(1 × 1) Surface. Journal of Physical Chemistry C, 2015, 119, 7809-7816.	1.5	11
61	Chemical Interaction, Space-Charge Layer, and Molecule Charging Energy for a TiO ₂ /TCNQ Interface. Journal of Physical Chemistry C, 2015, 119, 22086-22091.	1.5	9
62	Ortho and Para Hydrogen Dimers on G/SiC(0001): Combined STM and DFT Study. Langmuir, 2015, 31, 233-239.	1.6	12
63	Structural modifications of gold thin films produced by thiol-derivatized single-stranded DNA immobilization. Journal of Physics Condensed Matter, 2014, 26, 055010.	0.7	6
64	Etching of Graphene in a Hydrogen-rich Atmosphere toward the Formation of Hydrocarbons in Circumstellar Clouds. Journal of Physical Chemistry C, 2014, 118, 26882-26886.	1.5	9
65	Antiphase Boundaries Accumulation Forming a New C ₆₀ Decoupled Crystallographic Phase on the Rutile TiO ₂ (110)-(1 × 1) Surface. Journal of Physical Chemistry C, 2014, 118, 27318-27324.	1.5	5
66	Mimicking Mars: A vacuum simulation chamber for testing environmental instrumentation for Mars exploration. Review of Scientific Instruments, 2014, 85, 035111.	0.6	22
67	Sublattice Localized Electronic States in Atomically Resolved Graphene-Pt(111) Edge-Boundaries. ACS Nano, 2014, 8, 3590-3596.	7.3	19
68	Graphene etching on SiC grains as a path to interstellar polycyclic aromatic hydrocarbons formation. Nature Communications, 2014, 5, 3054.	5.8	59
69	Vacancy formation on C60/Pt (111): unraveling the complex atomistic mechanism. Nanotechnology, 2014, 25, 385602.	1.3	25
70	Sequential formation of N-doped nanohelicenes, nanographenes and nanodomes by surface-assisted chemical (cyclo)dehydrogenation of heteroaromatics. Chemical Communications, 2014, 50, 1555.	2.2	23
71	Silicene versus two-dimensional ordered silicide: Atomic and electronic structure of Si- <mml:math xmlns:mml="http://www.w3.org/1998/Math/MathML"><mml:mrow><mml:mrow><mml:mo>(</mml:mo><mm Physical Review B, 2014, 89, .</mm </mml:mrow></mml:mrow></mml:math 	l:msqr t > <m< td=""><td>າml:ສອາ>19<</td></m<>	າml :ສ ອາ>19<
72	Imaging Molecular Orbitals of PTCDA on Graphene on Pt(111): Electronic Structure by STM and First-Principles Calculations. Journal of Physical Chemistry C, 2014, 118, 12782-12788.	1.5	48

#	Article	IF	CITATIONS
73	Tailored Formation of N-Doped Nanoarchitectures by Diffusion-Controlled on-Surface (Cyclo)Dehydrogenation of Heteroaromatics. ACS Nano, 2013, 7, 3676-3684.	7.3	52
74	Chemistry and temperature-assisted dehydrogenation of C60H30 molecules on TiO2(110) surfaces. Nanoscale, 2013, 5, 11058.	2.8	17
75	Physicochemical Characterization of <i>Acidiphilium</i> sp. Biofilms. ChemPhysChem, 2013, 14, 1237-1244.	1.0	5
76	Effect of van der Waals forces on the stacking of coronenes encapsulated in a single-wall carbon nanotube and many-body excitation spectrum. Carbon, 2013, 54, 113-123.	5.4	25
77	Solventâ€Induced Delamination of a Multifunctional Two Dimensional Coordination Polymer. Advanced Materials, 2013, 25, 2141-2146.	11.1	146
78	Commensurate Growth of Densely Packed PTCDI Islands on the Rutile TiO2(110) Surface. Journal of Physical Chemistry C, 2013, 117, 12639-12647.	1.5	21
79	Small Pt nanoparticles on the TiO2 (110)–(1×2) surface. Surface Science, 2013, 607, 159-163.	0.8	9
80	Valence band electronic structure characterization of the rutile TiO2 (110)-(1×2) reconstructed surface. Surface Science, 2013, 608, 92-96.	0.8	19
81	Role of the Anchored Groups in the Bonding and Self-Organization of Macrocycles: Carboxylic versus Pyrrole Groups. Journal of Physical Chemistry C, 2013, 117, 7661-7668.	1.5	8
82	van der Waals interactions mediating the cohesion of fullerenes on graphene. Physical Review B, 2012, 86, .	1.1	54
83	Coordinated H-Bonding between Porphyrins on Metal Surfaces. Journal of Physical Chemistry C, 2012, 116, 15378-15384.	1.5	15
84	Large-area high-throughput synthesis of monolayer graphene sheet by Hot Filament Thermal Chemical Vapor Deposition. Scientific Reports, 2012, 2, 682.	1.6	138
85	Graphene Functionalisation with a Conjugated Poly(fluorene) by Click Coupling: Striking Electronic Properties in Solution. Chemistry - A European Journal, 2012, 18, 4965-4973.	1.7	75
86	Weakly Interacting Molecular Layer of Spinning C ₆₀ Molecules on TiO ₂ (110) Surfaces. Chemistry - A European Journal, 2012, 18, 7382-7387.	1.7	26
87	New Insights into the Characterization of â€~Insoluble Black HCN Polymers'. Chemistry and Biodiversity, 2012, 9, 25-40.	1.0	35
88	Planar Growth of Pentacene on the Dielectric TiO ₂ (110) Surface. Journal of Physical Chemistry C, 2011, 115, 4664-4672.	1.5	40
89	Following the Metalation Process of Protoporphyrin IX with Metal Substrate Atoms at Room Temperature. Journal of Physical Chemistry C, 2011, 115, 6849-6854.	1.5	63
90	On-surface synthesis of cyclic organic molecules. Chemical Society Reviews, 2011, 40, 4578.	18.7	154

#	Article	IF	CITATIONS
91	Strain-Driven Moiré Superstructures of Epitaxial Graphene on Transition Metal Surfaces. ACS Nano, 2011, 5, 5627-5634.	7.3	155
92	On-surface molecular engineering. Nature Chemistry, 2011, 3, 11-12.	6.6	12
93	Surface assembly of porphyrin nanorods with one-dimensional zinc–oxygen spinal cords. CrystEngComm, 2011, 13, 5591.	1.3	8
94	Back Cover: Simulating the organicâ€molecule/metal interface TCNQ/Au(111) (Phys. Status Solidi B 9/2011). Physica Status Solidi (B): Basic Research, 2011, 248, .	0.7	20
95	STM study of C60 overlayers on Pt(111) surfaces. Vacuum, 2011, 85, 1059-1062.	1.6	3
96	Thermal behaviour of the O2/TiO2 (110)–(1Â×Â2) surface. Vacuum, 2011, 85, 1056-1058.	1.6	2
97	New results on thermal and photodesorption of CO ice using the novel InterStellar Astrochemistry Chamber (ISAC). Astronomy and Astrophysics, 2010, 522, A108.	2.1	127
98	Protection of chemolithoautotrophic bacteria exposed to simulated Mars environmental conditions. Icarus, 2010, 209, 482-487.	1.1	47
99	Spontaneous Discrimination of Polycyclic Aromatic Hydrocarbon (PAH) Enantiomers on a Metal Surface. Chemistry - A European Journal, 2010, 16, 13920-13924.	1.7	8
100	Electrochemical growth of Acidithiobacillus ferrooxidans on a graphite electrode for obtaining a biocathode for direct electrocatalytic reduction of oxygen. Biosensors and Bioelectronics, 2010, 26, 877-880.	5.3	113
101	Understanding atomic-resolved STM images on TiO ₂ (110)-(1 × 1) surface by DFT calculations. Nanotechnology, 2010, 21, 405702.	1.3	33
102	Fossilization of Acidophilic Microorganisms. Geomicrobiology Journal, 2010, 27, 692-706.	1.0	8
103	Interplay between Fast Diffusion and Molecular Interaction in the Formation of Self-Assembled Nanostructures of <i>S</i> -Cysteine on Au(111). Langmuir, 2010, 26, 4113-4118.	1.6	38
104	Metal-organic extended 2D structures: Fe-PTCDA on Au(111). Nanotechnology, 2010, 21, 305703.	1.3	20
105	Ordered Vacancy Network Induced by the Growth of Epitaxial Graphene on Pt(111). Physical Review Letters, 2010, 105, 216102.	2.9	70
106	Thermal Wet Decomposition of Prussian Blue: Implications for Prebiotic Chemistry. Chemistry and Biodiversity, 2009, 6, 1309-1322.	1.0	27
107	CH4/N2/H2-spark hydrophobic tholins: A systematic approach to the characterisation of tholins. Part II. Icarus, 2009, 204, 672-680.	1.1	30
108	Morphological Investigation of Mn ₁₂ Single-Molecule Magnets Adsorbed on Au(111). Langmuir, 2009, 25, 10107-10115.	1.6	9

#	Article	IF	CITATIONS
109	Ultraviolet Photostability of Adenine on Gold and Silicon Surfaces. Astrobiology, 2009, 9, 573-579.	1.5	7
110	Azafullerene-like Nanosized Clusters. ACS Nano, 2009, 3, 3352-3357.	7.3	11
111	Production of nanohole/nanodot patterns on Si(001) by ion beam sputtering with simultaneous metal incorporation. Journal of Physics Condensed Matter, 2009, 21, 224009.	0.7	34
112	SVis: A Computational Steering Visualization Environment for Surface Structure Determination. , 2009, , .		1
113	Nucleic acid interactions with pyrite surfaces. Chemical Physics, 2008, 352, 11-18.	0.9	19
114	Synthesis of cobalt ferrite core/metallic shell nanoparticles for the development of a specific PNA/DNA biosensor. Journal of Colloid and Interface Science, 2008, 321, 484-492.	5.0	128
115	CH4/N2/H2 spark hydrophilic tholins: A systematic approach to the characterization of tholins. Icarus, 2008, 198, 232-241.	1.1	27
116	Fullerenes from aromatic precursors by surface-catalysed cyclodehydrogenation. Nature, 2008, 454, 865-868.	13.7	291
117	Label-free detection of DNA hybridization based on hydration-induced tension in nucleic acid films. Nature Nanotechnology, 2008, 3, 301-307.	15.6	194
118	Silicon Surface Nanostructuring for Covalent Immobilization of Biomolecules. Journal of Physical Chemistry C, 2008, 112, 9308-9314.	1.5	22
119	Direct evidence of nanowires formation from a Cu(i) coordination polymer. Chemical Communications, 2008, , 945-947.	2.2	43
120	Nexafs Study of Nitric Oxide Layers Adsorbed from a Nitrite Solution onto a Pt(111) Surface. Journal of Physical Chemistry C, 2008, 112, 10161-10166.	1.5	5
121	Molecular Conformation, Organizational Chirality, and Iron Metalation of meso-Tetramesitylporphyrins on Copper(100). Journal of Physical Chemistry C, 2008, 112, 8988-8994.	1.5	64
122	LEED-IV study of the rutileTiO2(110)â^'1×2surface with a Ti-interstitial added-row reconstruction. Physical Review B, 2007, 75, .	1.1	27
123	Do peptide nucleic acids form self-assembled monolayers on pyrite surfaces?. Surface Science, 2007, 601, 4195-4199.	0.8	11
124	A DNA biosensor based on peptide nucleic acids on gold surfaces. Biosensors and Bioelectronics, 2007, 22, 1926-1932.	5.3	79
125	Structure of RutileTiO2(110)â^'(1×2): Formation ofTi2O3Quasi-1D Metallic Chains. Physical Review Letters, 2006, 96, 055502.	2.9	60
126	Surface characterization of sulfur and alkanethiol self-assembled monolayers on Au(111). Journal of Physics Condensed Matter, 2006, 18, R867-R900.	0.7	163

#	Article	IF	CITATIONS
127	Two-Site Adsorption Model for the (â^š3 × â^š3)-R30º Dodecanethiolate Lattice on Au(111) Surfaces. Journal of Physical Chemistry B, 2006, 110, 5586-5594.	1.2	63
128	Scanning tunneling and photoemission spectroscopies at the PTCDA/Au(111) interface. Organic Electronics, 2006, 7, 287-294.	1.4	108
129	Following the oxidation of yttrium silicide epitaxially grown on Si(111) by core level photoemission spectroscopy. Surface Science, 2006, 600, 841-846.	0.8	0
130	Ultra-thin Si overlayers on the TiO2 (110)-(1×2) surface: Growth mode and electronic properties. Surface Science, 2006, 600, 2696-2704.	0.8	12
131	Nanostructured Organic Material: From Molecular Chains to Organic Nanodots. Advanced Materials, 2006, 18, 2048-2052.	11.1	37
132	A chamber for studying planetary environments and its applications to astrobiology. Measurement Science and Technology, 2006, 17, 2274-2280.	1.4	29
133	Subsurface structure of epitaxial rare-earth silicides imaged by STM. Physical Review B, 2006, 74, .	1.1	24
134	Nucleic Acids and Their Analogs as Nanomaterials for Biosensor Development. Current Nanoscience, 2006, 2, 257-273.	0.7	24
135	Bottom-Up Fabrication of Carbon-Rich Silicon Carbide Nanowires by Manipulation of Nanometer-Sized Ethanol Menisci. Advanced Materials, 2005, 17, 1480-1483.	11.1	61
136	Structural and functional characterization of self-assembled monolayers of peptide nucleic acids and its interaction with complementary DNA. Journal of Molecular Catalysis A, 2005, 228, 131-136.	4.8	20
137	Surface atomic structure determination of three-dimensional yttrium silicide epitaxially grown on Si(111). Physical Review B, 2005, 71, .	1.1	14
138	Self-Assembled Monolayers of Peptide Nucleic Acids on Gold Surfaces:Â A Spectroscopic Study. Langmuir, 2005, 21, 9510-9517.	1.6	54
139	Electronic structure and Fermi surface of two-dimensional rare-earth silicides epitaxially grown on Si(111). Physical Review B, 2004, 69, .	1.1	40
140	Ordered Self-Assembled Monolayers of Peptide Nucleic Acids with DNA Recognition Capability. Physical Review Letters, 2004, 93, 208103.	2.9	42
141	Metal release in metallothioneins induced by nitric oxide: X-ray absorption spectroscopy study. European Biophysics Journal, 2004, 33, 726-731.	1.2	5
142	A study of the formation of yttrium silicides epitaxially grown on Si(111). Surface and Interface Analysis, 2004, 36, 1195-1198.	0.8	5
143	Sulfur electroadsorption on Au(111). Electrochimica Acta, 2004, 49, 3643-3649.	2.6	25
144	Use of angle-resolved photoemission and density functional theory for surface structural analysis of YSi2. Surface Science, 2004, 566-568, 1047-1051.	0.8	4

#	Article	IF	CITATIONS
145	Growth of subnanometer-thin Si overlayer on TiO2 (110)-(1×2) surface. Applied Surface Science, 2004, 234, 497-502.	3.1	13
146	Cyclic Voltammetry and Structural Studies of Nitric Oxide Monolayers Adsorbed on Pt(111). Electroanalysis, 2003, 15, 726-732.	1.5	2
147	Following Adsorption Kinetics at Electrolyte/Metal Interfaces through Crystal Truncation Scattering: Sulfur on Au(111). Physical Review Letters, 2003, 90, 075506.	2.9	34
148	XPS and AFM Characterization of Oligonucleotides Immobilized on Gold Substrates. Langmuir, 2003, 19, 6230-6235.	1.6	42
149	Patterson function from low-energy electron diffraction measured intensities and structural discrimination. Physical Review B, 2003, 67, .	1.1	7
150	Diffusion and nucleation of yttrium atoms on Si(111)7×7: A growth model. Physical Review B, 2002, 66, .	1.1	34
151	Structural determination of two-dimensionalYSi2epitaxially grown on Si(111). Physical Review B, 2002, 66, .	1.1	26
152	Nitric-oxide adsorption and oxidation on Pt() in electrolyte solution under potential control. Surface Science, 2002, 507-510, 688-694.	0.8	21
153	Structural and optical characterization of WO3 deposited on glass and ITO. Vacuum, 2002, 64, 287-291.	1.6	37
154	Chromium-based thin sputtered composite coatings for solar thermal collectors. Vacuum, 2002, 64, 299-305.	1.6	12
155	Compositional characterization of silicon nitride thin films prepared by RF-sputtering. Vacuum, 2002, 67, 513-518.	1.6	9
156	Deposition of PVD solar absorber coatings for high-efficiency thermal collectors. Vacuum, 2002, 67, 623-627.	1.6	33
157	Sulfurâ^'Substrate Interactions in Spontaneously Formed Sulfur Adlayers on Au(111). Langmuir, 2001, 17, 4919-4924.	1.6	107
158	A photoemission study of the SO2 adsorption on TiO2 (110) surfaces. Surface Science, 2001, 482-485, 9-14.	0.8	34
159	Surface morphology of yttrium silicides epitaxially grown on Si(111) by STM. Surface Science, 2001, 482-485, 1337-1342.	0.8	18
160	Adsorption and desorption ofSO2on theTiO2(110)â^'(1×1)surface: A photoemission study. Physical Review B, 2001, 64, .	1.1	62
161	Spectrally selective composite coatings of Cr–Cr2O3 and Mo–Al2O3 for solar energy applications. Thin Solid Films, 2001, 392, 320-326.	0.8	123
162	Structure of Si atomic chains grown on the Si/Cu(110)c(2×2)surface alloy. Physical Review B, 2001, 63, .	1.1	18

#	Article	IF	CITATIONS
163	Formation of the Si/Cu interface. Surface and Interface Analysis, 2000, 30, 570-573.	0.8	3
164	Formation and stability of the Cu(110)+c(2×2)-Si surface alloy studied by high resolution XPS. Surface Science, 2000, 454-456, 778-782.	0.8	11
165	The Y–Si(111) interface formation studied by scanning tunneling microscopy. Surface Science, 2000, 454-456, 842-846.	0.8	4
166	Electronic structure and nature of the bonding at the Cu(110)+c(2×2)-Si surface alloy. Surface Science, 2000, 466, 144-154.	0.8	14
167	Atomic origin of the Si core-level photoemission components in theC(2×2)Si-Cu(110) surface alloy. Physical Review B, 1999, 59, 3070-3074.	1.1	23
168	Oxygen Induced Reconstruction of the Rh(100) Surface: General Tendency Towards Threefold Oxygen Adsorption Site on Rh Surfaces. Physical Review Letters, 1999, 82, 4874-4877.	2.9	54
169	Study of the electronic bonding of Cl–Si(100) by synchrotron radiation photoemission spectroscopy and many-body calculations. Surface Science, 1999, 424, 82-93.	0.8	9
170	A photoelectron diffraction method to evaluate in-plane atomic distances at surfaces: the two atoms approximation. Surface Science, 1999, 429, 298-308.	0.8	2
171	STM studies of the growth of the Si/Cu(110) surface alloy. Surface Science, 1998, 402-404, 245-248.	0.8	26
172	LEED structural determination of the c(2 $ ilde{A}$ — 2) surface alloy. Surface Science, 1998, 407, 268-274.	0.8	20
173	Semiconductor-metal transition of the single-domainK/Si(100)â^'(2×1)interface by Fermi-surface determination. Physical Review B, 1998, 57, 9201-9207.	1.1	8
174	Origin of the buckling in thec(2×2)-Si/Cu(110) surface alloy. Physical Review B, 1998, 57, 4493-4499.	1.1	14
175	Si intralayers at GaAs/AlAs and GaAs/GaAs junctions: Polar versus nonpolar interfaces. Physical Review B, 1998, 57, 12314-12323.	1.1	11
176	Highly homogeneous nanoparticulate Fe films prepared by laser ablation. IEEE Transactions on Magnetics, 1998, 34, 1108-1110.	1.2	4
177	Surface character in the experimental Fermi surface of epitaxialErSi1.7s(0001) by photoemission spectroscopy. Physical Review B, 1997, 55, 5129-5135.	1.1	3
178	Surface atomic structure of c(2×2)-Si on Cu(110). Physical Review B, 1997, 55, 12896-12898.	1.1	28
179	Surface damage in the submonolayer growth of carbon on Si(111)7×7 by means of the laser ablation deposition technique. Journal of Vacuum Science and Technology A: Vacuum, Surfaces and Films, 1997, 15, 39-42.	0.9	2
180	Surface atomic structure of epitaxially grown erbium silicide films on Si(111)7×7. Physical Review B, 1997. 55. 5136-5140.	1.1	30

#	Article	IF	CITATIONS
181	STRUCTURAL DETERMINATION OF THE Si/Cu(110) INTERFACE BY PHOTOELECTRON DIFFRACTION. Surface Review and Letters, 1997, 04, 1331-1335.	0.5	1
182	Chemical and Morphological Changes of the Pyrite Induced by Leaching and Bioleaching Processes in the Presence of Catalytic Ag Ions. Langmuir, 1997, 13, 3355-3363.	1.6	6
183	Experimental Fermi surface determination of epitaxial ErSi1.7(0001) on Si(111). Surface Science, 1997, 377-379, 172-176.	0.8	0
184	The valence-band electronic structure of clean and Pt-covered TiO2(110) surfaces studied with photoemission spectroscopy. Journal of Electron Spectroscopy and Related Phenomena, 1997, 83, 217-225.	0.8	15
185	Study of the interaction of SO2 with TiO2 (110) surface. Vacuum, 1997, 48, 597-600.	1.6	27
186	The interaction of Pt with TiO2(110) surfaces: a comparative XPS, UPS, ISS, and ESD study. Surface Science, 1996, 345, 261-273.	0.8	208
187	Growth and morphology of epitaxial ErSi1.7 films on Si(111) 7 × 7 studied by scanning tunneling microscopy. Surface Science, 1996, 366, 491-500.	0.8	27
188	Evidence of an implantation process in carbon deposition on Si(100) at high substrate temperature by laser ablation. Surface Science, 1996, 369, 45-50.	0.8	1
189	As and Ga dimers in coreâ€level spectroscopy of Sâ€passivated GaAs(001). Journal of Applied Physics, 1996, 80, 5372-5376.	1.1	7
190	Direct evidence of occupied states near the Fermi level on the Si(100) 2 × 1-K interface. Surface Science, 1994, 307-309, 995-1000.	0.8	10
191	STM studies of Si evaporation on Si at RT by laser ablation. Surface Science, 1993, 287-288, 911-914.	0.8	1
192	Electron loss spectroscopy study of the growth by laser ablation of ultra-thin diamond-like films on Si(100). Surface Science, 1992, 260, L17-L23.	0.8	21
193	Raman spectroscopy of carbon films grown by pulsed laser evaporation of graphite. Diamond and Related Materials, 1992, 1, 824-827.	1.8	29
194	Epitaxial growth of diamond-like films on Si(100) by pulsed-laser evaporation of graphite. Materials Science and Engineering B: Solid-State Materials for Advanced Technology, 1992, 11, 337-340.	1.7	8
195	Scanning tunnelling microscopy studies of diamond-like films prepared by laser ablation. Materials Science and Engineering B: Solid-State Materials for Advanced Technology, 1992, 11, 363-367.	1.7	1
196	Scanning tunneling microscopy observation of the initial stages of growth of carbon films grown by pulsed laser vaporization of graphite. Ultramicroscopy, 1992, 42-44, 616-623.	0.8	7
197	Epitaxial growth of crystalline, diamondâ€like films on Si (100) by laser ablation of graphite. Applied Physics Letters, 1990, 57, 1742-1744.	1.5	65